

# Impact of Photovoltaic Plant Outputs in Distribution Networks

Abid Ali Jamali<sup>1,\*</sup>, Nursyarizal Mohd Nor<sup>1</sup>, Taib Ibrahim<sup>1</sup>, Mohd Fakhizan Romlie<sup>1</sup>, and Zahid Khan<sup>2</sup>

<sup>1</sup>Department of Electrical and Electronics Engineering, Universiti Teknologi PETRONAS, Bandar Seri Iskandar, Malaysia.

<sup>2</sup> Department of Fundamental and Applied Sciences, Universiti Teknologi PETRONAS, Bandar Seri Iskandar, Malaysia

**Abstract.** This paper evaluates the potential of Quaid-e-Azam Solar Park (QASP), Pakistan and examines its impact on distribution networks. To estimate the PV plant yields, solar park's historical hourly weather data from the years 2000 - 2014 is used. For handling of such huge data, the yearly data is partitioned into four seasons. Further, the seasonal data is modelled by using Beta Probability Density Function (PDF) and a 24 hour solar curve for each season is generated. The solar farm power outputs are tested in IEEE 33 bus distribution network by using time-varying seasonal hourly loads, meanwhile system losses and bus voltages are calculated. The results show that with the passage of time, the impact of solar PV power on reduction of system losses gradually decrease due to yearly degradation of PV module efficiency. System losses at end of PV farm life are 10 - 12% higher than those losses as in the first year. Furthermore, low voltage buses also pose to risk as system voltages also start to decrease. From the analysis, it is suggested that for maintaining the quality of network, time varying detailed assessments should be performed during the calculations of sizing of distributed generation.

## 1 Introduction

Renewable energy has been considered as a key solution for producing electricity in coming years. Various renewable energy technologies such as large wind farms, biomass, solar photovoltaic and thermal plants and hydroelectric power plants, are emerging and are widely available now, ranging from small to large scale in megawatt sizes. However, intermittencies of renewable sources such as wind speeds and solar irradiations, are yet major obstacles and are limiting their utilization with a condition of proper planning. Research shows that installation of renewable energy sourced Distributed Generations (DGs) into grid without planning may worsen the power quality rather than giving benefits to distribution networks. Research suggests that DGs with known sizes must be installed at proper locations in order to keep the system performance maintained. However, during the literature review [1-7], it is noticed that actual sources of real and reactive powers are not well defined by many

---

\* Corresponding author: [powereng1982@gmail.com](mailto:powereng1982@gmail.com)

authors. Availability of local resources and characteristics of weather data directly affect the plant outputs. Therefore, considering renewable power sources without dealing with weather statistics may pose risk to grid operations.

Moreover, in many developing and under-developed countries, electricity demand and generation balance is a major issue and with passage of time, it is getting more worsened. Pakistan is facing the electricity generation deficit of more than 20 % as per government authorities and media resources [8]. As of now, the country is inviting investors to invest in developing power plants by using Renewable Energy Sources (RES) and in that regards, competitive tariffs for wind farms and solar PV plants have been advertised publically [9]. Initiatives have already been taken by the authorities by reserving government land in high wind areas at Jhimpir, Pakistan’s wind corridor, for building large size wind farms. Moreover, in addition to various small scale solar PV systems, installed by residual users and land farmers, the country is developing its 1000 megawatt solar PV plant, at Bahawalpur, named as Quaid-e-Azam Solar Park (QASP). The QASP is claimed to be Asia’s largest solar farm and is being developed in phases. As of now, 100 MW size PV modules are already installed and its produced electricity is being dispatched to grid via a 132 kV substation [10].

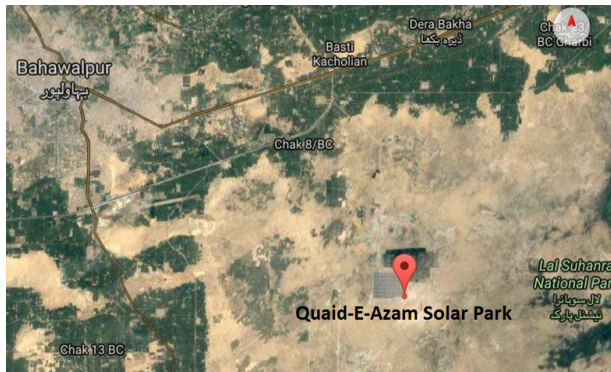


**Fig. 1.** Location of solar PV farm for the study.

The preliminary site assessment results submitted for this solar farm to National Electric Power Regulatory Authority (NEPRA) are provided in **Error! Reference source not found.** [11]. However, impacts of solar PV farm on distributed network due to varying demand and varying power outputs, are undetermined.

**Table 1.** Quaid-e-Azam Solar Park actual site results.

S.no	Description	Value
1	Total installed capacity of PV plant	100 MWp DC
2	Type of PV module	Polycrystalline
3	Inverter conversion efficiency	98.5 %
4	Average daily sunny hour	5.18
5	Annual PV Plant generation capacity (simulation)	160,313 MWh
6	Expected total energy generation in 25 years life span	3,727,586 MWh
7	Net capacity factor	18.30%

This paper evaluates the potential of Quaid-e-Azam Solar Park (QASP) and its impact on distribution network using historical hourly weather data of last 15 years. The weather data for the solar park is available online at National Solar Radiation Database (NSRDB) [12].

For handling of such huge data, the yearly data is partitioned into 4 seasons, each season consists yearly data of specified three months. Then seasonal data is processed by using Beta Probability Density Function (PDF) and a 24 hour solar curve for each season is generated. IEEE 33 bus distribution system is considered for testing of solar park outputs. For ease of simulation, the size of PV farm is considered between 2.48 – 2.6 MW and farm location is chosen as bus No.6, based on the literature review available for IEEE 33 bus distribution system. Moreover, the paper is organized as follows: Section 2 covers the problem formulation, solar PV modelling and calculations for PV module output, load modelling, mathematical equation of PV farm power injection and system loss calculation with and without PV power. In section 3 contains the simulation results and step-by-step discussion. In last section, simulation results are summarized.

## 2 Problem Formulation

### 2.1 Solar PV Modelling

There are two methods that are commonly used to harvest the energy from solar light and these are known as solar thermal and PV technology. The first technology uses thermal collectors to collect the heat from solar light, the heat is then used for different heating processes at power plants as well as heating in general at different industries. In second option, solar photovoltaic (PV) modules are used which directly convert the sun light into electricity. The PV technology is getting more popularity mainly due to its reduced cost and size, installation methods, required equipment, and increasing efficiency. Before installing PV modules, it is very important to know the weather statistics of the proposed location. Normally large PV plants are installed at higher irradiant areas, however, ambient temperature of the location negatively affects the outputs of PV module. Therefore, sunny areas with low temperature are more favorable than sunny areas with higher temperature within same country.

Output of PV module is a function of meteorological conditions such as solar light and ambient temperature. So it becomes necessary to evaluate the regional weather conditions before installation of PV plants. For the feasibility of PV plant locations, there are various statistical models such as Beta PDF that is used to model the daily solar irradiance. This solar probability model has been considered in many solar PV studies [13-17]. These probability density function use hourly historical data as input and easily calculate the probability of occurrence of a range of possible values.

To describe the random phenomenon of solar irradiance, the weather data of each year is divided into four seasons and each season represents the combinational data of three months. Then based on the probabilistic modelling, the seasonal three months data is converted into equivalent 24 samples. So by end of data assessment, we will get  $4 \times 24 = 96$  samples.

The Beta PDF for solar irradiance for each hour can be expressed as follows:

$$\begin{aligned} & \text{Beta}(s) \\ &= \begin{cases} \frac{\Gamma(\alpha + \beta)}{\Gamma(\alpha)\Gamma(\beta)} s^{(\alpha-1)}(1-s)^{(\beta-1)}, & 0 \leq s \leq 1, \alpha, \beta \geq 0 \\ 0 & \text{otherwise} \end{cases} \end{aligned} \tag{1}$$

where  $\text{beta}(s)$  is the Beta distribution function of  $s$ ,  $s$  is the irradiance of solar light in kW/m, whereas  $\alpha$  and  $\beta$  are two input parameters of  $\text{beta}(s)$ , which are calculated with the help of mean ( $\mu$ ) and standard deviation ( $\sigma$ ) of seasonal hourly solar irradiance and are given by as followings:

$$\beta = (1 - \mu) \left( \frac{\mu(1 + \mu)}{\sigma^2} - 1 \right)$$

$$\alpha = \frac{\mu X \beta}{1 - \mu}$$

The probability of the solar irradiance state during any specific hour can be calculated from (3) as follows [14, 17]:

$$p(s) = \int_{s_1}^{s_2} \text{beta}(s) ds \tag{2}$$

where  $s_1$  and  $s_2$  are solar irradiance limits of state.

## 2.2 PV Module Output

The peak power of a PV module is a function of PV cells, connected in series and parallel, depending on system voltage and current requirements. The peak power of a PV module is measured in watts and it is equal to the maximum power of module's output under the standard test conditions. Normally the characteristics of PV module are provided in form of following parameters. [14, 17]

- $I_{sc}$  (Short circuit current in A),
- $V_{oc}$  (Open-circuit voltage in V),
- $I_{MPP}$  (Current at maximum power point in A),
- $V_{MPP}$  (Voltage at maximum power point in V),
- $NOCT$  (Nominal operating temperature of cell in °C)
- $K_v$  (Voltage temperature coefficients in V/°C)
- $K_i$  (Current temperature coefficients in A/°C)

The short circuit current is directly proportional to the solar irradiations, whereas the voltage is inversely proportional to the temperature. So from that statement, it is understood that sunny regions are not always good to install PV systems, as increasing temperature will intensely reduce the output of PV modules. To cope voltage and current relationship, PV modules are equipped with Maximum Power Point Trackers (MPPT), which help to provide maximum power by matching module's V-I characteristics. The power output of PV module during a time segment ( $h$ ), can be measured by using following equations [14, 17]

$$PV_{OUT}(h) = \int_0^1 PV_{NET} p(s) ds \tag{3}$$

$$PV_{NET} = FF \times V_{NET} \times I_{NET}$$

$$FF = \frac{V_{MPP} \times I_{MPP}}{V_{OC} \times I_{SC}}$$

$$V_{NET} = V_{OC} - K_v \times T_c$$

$$I_{NET} = s[I_{SC} + K_i \times (T_c - 25)]$$

$$T_c = T_A + s \left( \frac{(NOCT - 20)}{0.8} \right)$$

where  $T_c$  and  $T_A$  are cell and ambient temperatures (°C), respectively and  $FF$  is the fill factor.

### 2.3 Load Model

For simulation purpose, four typical daily load profile using IEEE-RTS load data as in [14], are used and each of these load profile represent load for each season.

**Table 2.** Parameters.

Hour	Seasons			
	1	2	3	4
1	0.67	0.63	0.64	0.63
2	0.63	0.62	0.6	0.62
3	0.6	0.6	0.58	0.6
4	0.59	0.58	0.56	0.58
5	0.59	0.59	0.56	0.59
6	0.6	0.65	0.58	0.65
7	0.74	0.72	0.64	0.72
8	0.86	0.85	0.76	0.85
9	0.95	0.95	0.87	0.95
10	0.96	0.99	0.95	0.99
11	0.96	1	0.99	1
12	0.95	0.99	1	0.99
13	0.95	0.93	0.99	0.93
14	0.95	0.92	1	0.92
15	0.93	0.9	1	0.9
16	0.94	0.88	0.97	0.88
17	0.99	0.9	0.96	0.9
18	1	0.92	0.96	0.92
19	1	0.96	0.93	0.96
20	0.96	0.98	0.92	0.98
21	0.91	0.96	0.92	0.96
22	0.83	0.9	0.93	0.9
23	0.73	0.8	0.87	0.8
24	0.63	0.7	0.72	0.7

Practically, electrical demand increases each year as a percentage of peak load, however, as a limitation of study, the load of each season throughout the simulation will remain same. The hourly load is varying from 0.59 p.u. to 1 p.u., 0.58 p.u. to 1 p.u., 0.56 p.u. to 1 p.u., and 0.58 p.u. to 1 p.u., in winter, spring, summer and fall, respectively. The load factor of the system is 0.87 p.u. is same for all four seasons.

### 2.4 PV Power Injection into Grid

Total active and reactive power injections at bus 6 where the PV farm output is installed, are respectively given as followings [17].

$$P_6 = P_{PV} - P_{D6} \tag{4}$$

$$Q_6 = Q_{PV} - Q_{D6}$$

Since  $Q_{PV}$  is a function of  $P_{PV}$  with a fixed power factor, therefore:

$$Q_6 = aP_{PV6} - Q_{D6} \tag{5}$$

where, P6 and Q6 are respectively the active and reactive power injections from the PV inverter at bus 6, and,

$$a = \pm \tan(\cos^{-1}(pf(PV_6)))$$

When sign = +1: the inverter is injecting reactive power, sign = -1: the inverter is consuming reactive power; PD<sub>6</sub> and QD<sub>6</sub> are the active and reactive power of the bus loads, where pf is the operating power factor of the inverter. Since PV power is known as only a source of active power, therefore unity power factor is considered for inverter output.

### 2.5 Power Loss

For calculating the active and reactive power losses across the distribution lines, exact loss formula has been used. The sum of active and reactive power losses of all buses in the distribution system are given as [17]:

$$P_{Li} = \sum_{i=1}^N \sum_{j=1}^N [\alpha_{ij}(P_i P_j + Q_i Q_j) + \beta_{ij}(Q_i P_j - P_i Q_j)] \tag{6}$$

$$Q_{Li} = \sum_{i=1}^N \sum_{j=1}^N [\gamma_{ij}(P_i P_j + Q_i Q_j) + \xi_{ij}(Q_i P_j - P_i Q_j)] \tag{7}$$

where,

$$\alpha_{ij} = \frac{r_{ij}}{V_i V_j} \cos(\delta_i - \delta_j), \beta_{ij} = \frac{r_{ij}}{V_i V_j} \sin(\delta_i - \delta_j)$$

$$\gamma_{ij} = \frac{x_{ij}}{V_i V_j} \cos(\delta_i - \delta_j), \xi_{ij} = \frac{x_{ij}}{V_i V_j} \sin(\delta_i - \delta_j)$$

$V \angle \delta$  is the complex bus voltages, r and x are the element of impedance matrix, P<sub>i</sub> and P<sub>j</sub>, Q<sub>i</sub> and Q<sub>j</sub> are active and reactive power injections at buses i and j, respectively. The system active and reactive power losses with PV power can be calculated by substituting equations (1) and (2) into equations (3) and (4), hence with substitution, we obtained the following formulas:

$$P_{LPVi} = \sum_{i=1}^N \sum_{j=1}^N \left[ \alpha_{ij}((P_{PVi} - P_{Di})P_j + (\alpha_i P_{PVi} - P_{Di})Q_j) + \beta_{ij}((\alpha_i P_{PVi} - P_{Di})P_j - (P_{PVi} - P_{Di})Q_j) \right] \tag{8}$$

$$Q_{LPVi} = \sum_{i=1}^N \sum_{j=1}^N \left[ \gamma_{ij}((P_{PVi} - P_{Di})P_j + (\alpha_i P_{PVi} - P_{Di})Q_j) + \xi_{ij}((\alpha_i P_{PVi} - P_{Di})P_j - (P_{PVi} - P_{Di})Q_j) \right] \tag{9}$$

### 2.6 Test System

The 33-bus test radial distribution test system as shown in Fig. 2 is used for the simulations purpose. The active and reactive demand of the system is 3.71 MW and 2.3 MVar, respectively. The total real and reactive losses of the base case system are known to be 211 kW and 143 kVAr [18-20]. The distribution network's line and load data are available in [21]. For calculating the load flow in distribution network, the Backward-Forward Sweep method [4, 18] is used.

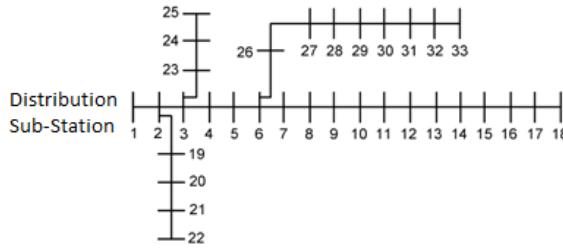


Fig. 2. **Schematic.**

Data in Table 3 shows some references that have been considered for sizing and location of PV farm installation for this study. For simulation purpose, we will choose a random number from the range of DG sizes, proposed for the IEEE 33 distribution network.

**Table 3.** Distribution generation data for validation.

Reference	Tested system	DG Bus No.	DG Size	Losses
			MW	kW
Acharya et al.[1]	33 and 69	6 and 61	2.49 and 1.81	111.24 and 81.44
Duong et al. [22]	33	6	2.6	111.1
Tuba et al. [23]	69	61	1.81	92

### 3 Simulation Results and Discussion

The mean ( $\mu$ ) and standard deviation ( $\sigma$ ) of the historical solar irradiance data is provided in Table 4. Further, by using equations (3) and (4), the Beta Probability Density Function (PDF) for 20 solar irradiance states with an interval of 0.05 kW/m<sup>2</sup> for the hour No. 10, 14, and 18 for each season is generated and plotted in Fig. 3 – Fig 6.

**Table 4.** Mean and standard deviation of historical solar data.

H. No	Season 1		Season 2		Season 3		Season 4	
	$\mu$	$\sigma$	$\mu$	$\sigma$	$\mu$	$\sigma$	$\mu$	$\Sigma$
8	0.00	0.00	0.03	0.02	0.01	0.01	0.00	0.00
9	0.02	0.03	0.17	0.04	0.14	0.03	0.03	0.04
10	0.16	0.08	0.37	0.06	0.33	0.05	0.19	0.07
11	0.35	0.11	0.56	0.07	0.51	0.07	0.37	0.09
12	0.51	0.14	0.72	0.09	0.67	0.09	0.52	0.10
13	0.63	0.17	0.84	0.09	0.78	0.11	0.62	0.10
14	0.69	0.17	0.88	0.10	0.82	0.12	0.65	0.10
15	0.69	0.16	0.86	0.09	0.79	0.13	0.62	0.10
16	0.61	0.15	0.77	0.09	0.71	0.13	0.53	0.09
17	0.48	0.13	0.63	0.08	0.57	0.12	0.38	0.07
18	0.31	0.10	0.45	0.07	0.40	0.09	0.19	0.06
19	0.11	0.07	0.25	0.05	0.21	0.07	0.02	0.03
20	0.00	0.01	0.07	0.03	0.05	0.04	0.00	0.00
21	0.00	0.00	0.00	0.00	0.00	0.00	0.00	0.00

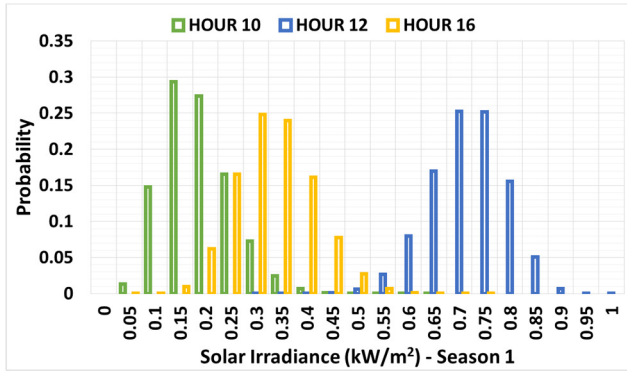


Fig. 3. Solar Irradiance probability for season 1.

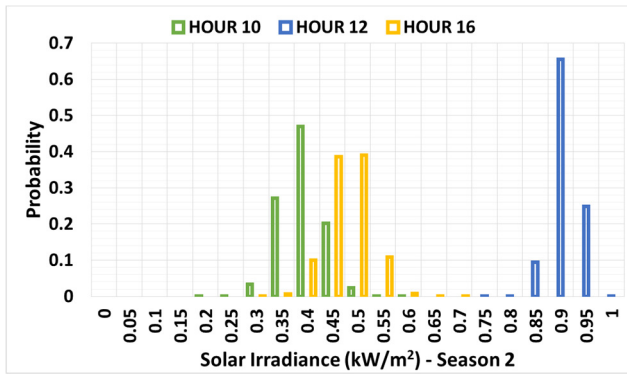


Fig. 4. Solar Irradiance probability for season 2.

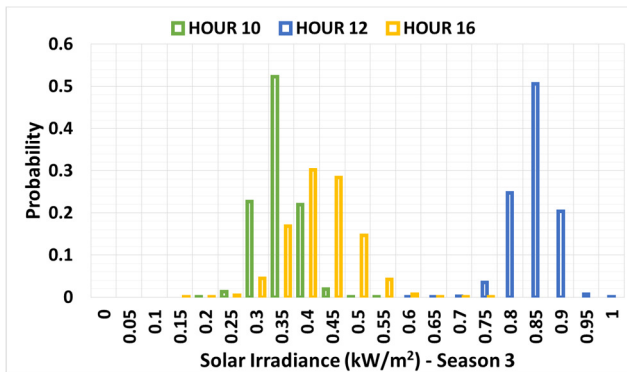
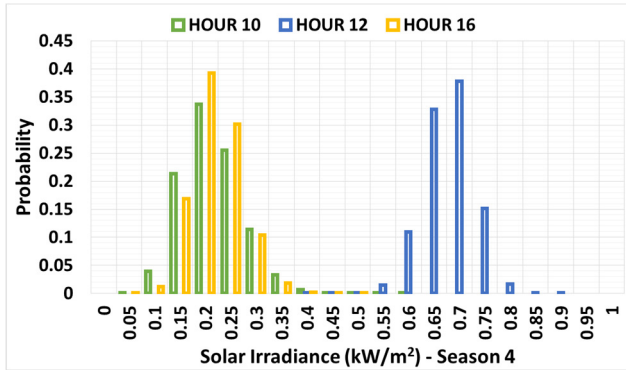
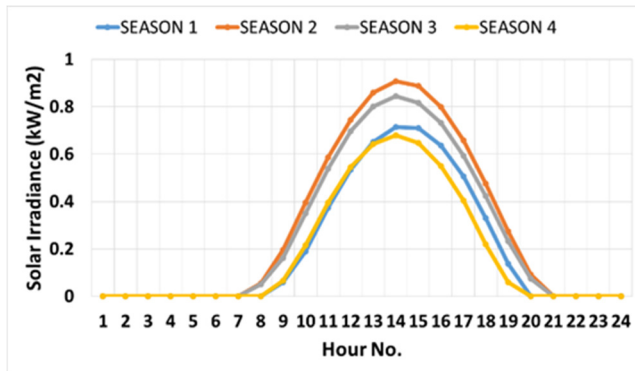


Fig. 5. Solar Irradiance probability for season 3.



**Fig. 6.** Solar Irradiance probability for season 4.

Using the Beta PDF values, the normalized expected daily solar radiations for all seasons are calculated and plotted in Fig. 7. The daily average ambient temperature of the four seasons are plotted in Fig. 8. Table 5 shows the technical specifications of the PV module, which is used and installed at QASP and same specifications values are considered for this study. The module has a peak output rating of 250 watt under standard test conditions. By using the seasonal expected daily solar irradiances and seasonal average ambient temperature, the expected seasonal power outputs from a PV module are calculated and are plotted in Fig. 9.



**Fig. 7.** Normalized daily expected solar PV output.

In the plots as in Fig. 7, solar irradiances starts to receive from 7<sup>th</sup> hour to 21<sup>st</sup> hour during summer and from 9<sup>th</sup> hour to 20<sup>th</sup> hour in winter. Maximum irradiances during summer may go beyond 900 watts/m<sup>2</sup> but in winter, irradiances are as lower as 650 watts/m<sup>2</sup>. Overall, the farm site receives 4.4 - 6.9 peak sunny hours (PSH) through the year.

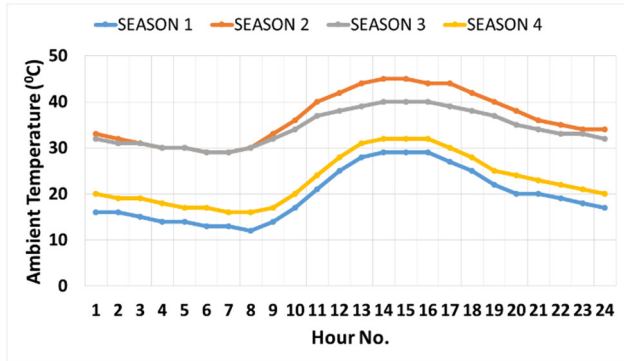


**Fig. 8.** Seasonal ambient temperature.

The site temperature is ranging from 30-45 °C in summer and 12-30 °C in other months. The higher temperature during summer are not good for the solar farm and definitely will cause to reduce the PV module outputs.

**Table 5.** Seasonal ambient temperature.

Nominal operating temperature of cell (NOCT)	44 0C
Current at maximum power point (IMPP)	8.28 A
Voltage at maximum power point (VMPP)	30.2 V
Short-circuit Current (ISC)	8.7 A
Open-circuit voltage (VOC)	37.6 V
Current temperature coefficients (Ki)	0.0045
Voltage temperature coefficients (Kv)	0.1241

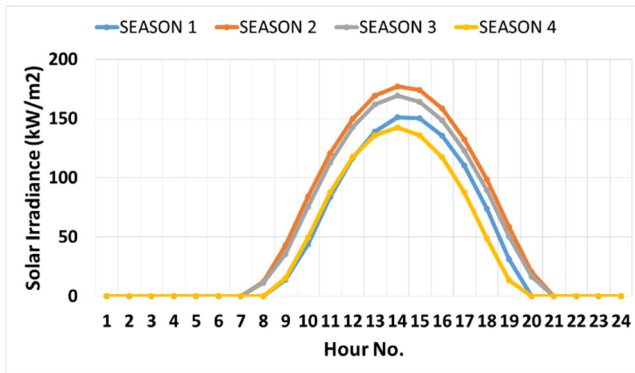


**Fig. 9.** Expected output from the chosen PV module.

In the Fig. 9, it can be observed that a PV module can produce 151 watts, 177 watts, 169 watts and 142 watts in season 1, 2, 3 and season 4, respectively. These lower output results clearly highlight the adverse effects of higher temperatures.

During the simulation, the size of PV farm was randomly chosen as 2.48 MWp and using farm site weather data, seasonal real energy losses with and without PV farm for the first year and 25<sup>th</sup> year are calculated by using (3) and are plotted in Fig. 10. Based on previous literature as provided in in Table 3, bus No.6 was chosen as the location of PV farm.

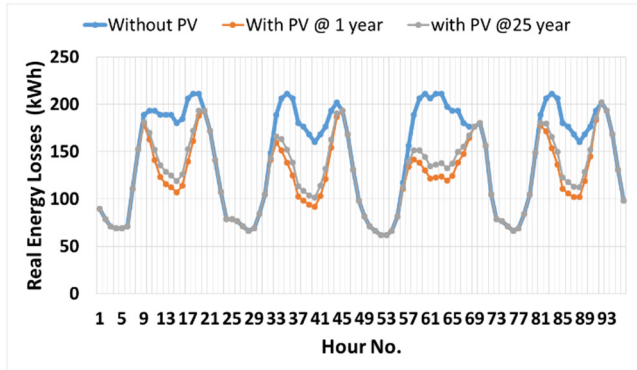


**Fig. 10.** Seasonal real energy losses with and without PV.

The real energy losses of the peak loaded hour during the first year are ranging between 122 kW to 187 kW, while in literature, real power losses during peak load hours are known to be 111 kW for IEEE 33 bus system, using the same size of DG [1, 22]. The real energy losses of the peak loaded hour during the 25<sup>th</sup> year are ranging between 136 kW to 193 kW, this shows that by the passage of time, the impact of solar PV power on reduction of system losses will gradually decrease due to lower PV outputs. The minimum system voltage with and without PV farm are plotted in Fig. 11. The figure shows the minimum bus voltages for base case and compare them with minimum voltages during first and 25<sup>th</sup> year of PV farm. Moreover, this impact will be higher when load increments are also considered for each year. In next 25 years, the network demand will be much higher than that what it is now. The changes in PV output from first to 25<sup>th</sup> year can be noticed in Fig. 12, which shows that about 10 - 12 % of system losses will revert back by end of solar PV farm life.

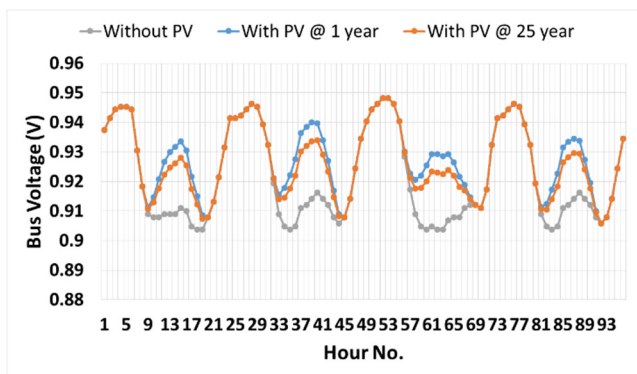


**Fig. 11.** Minimum system voltage during 25th year.

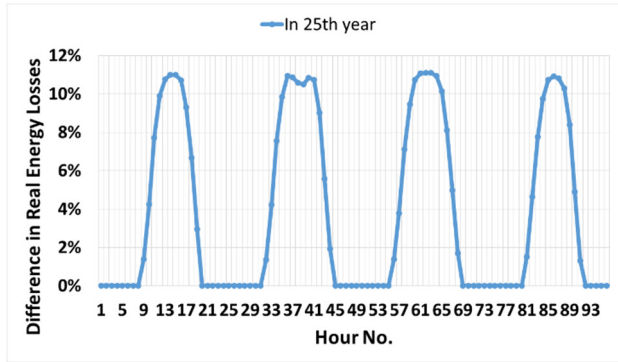


**Fig. 12.** Difference of system losses in first and 25th year.

Fig. 11 summarizes the system losses with and without PV farm and compares the seasonal losses in base case and losses with addition of PV farm during the 25 year life. The reduction in system losses with and without PV farm is about 16%.

**Table 6.** Summary of system losses with and without PV farm.

Season	Real Power Losses (MWh)		
	Base case	With PV	% Reduction
1	7967.088	6762.322	15%
2	8112.743	6601.361	19%
3	8092.739	6581.17	19%
4	8112.743	7016.328	14%
Total	32285.31	26961.18	16%

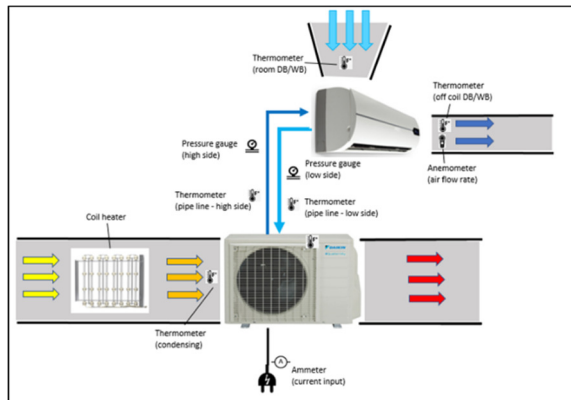


**Fig. 13.** Schematic.

**Table 7.** Parameters.

Refrigerant charge, [%]	80, 85, 90, 95, 100, 105, 110, 115, 120
Outdoor temperature, $T_o$ [°C]	30

$$C_T = VFR \times \rho_{air} \times \Delta h \tag{10}$$

## 4 Conclusion

Through this paper, the potential of Quaid-e-Azam Solar Park (QASP), Pakistan, was evaluated and the impact of the solar park power output was examined on the time varying load models in the distribution network. Fifteen years' historical satellite weather data of the solar park location was used and a daily solar irradiation curve for each season was generated by using Beta Probability Density Function (PDF). From the results, it was known that by the passage of time, the impact of solar PV power on reduction of system losses will gradually decrease due to lower PV outputs and system losses at end of PV farm life will be 10 - 12% higher than those as during the first year. Moreover, weaker bus with low voltage would also pose to risk as system voltage gradually started to decrease. From the analysis, it is suggested that for maintaining the quality of network, time varying detailed assessments should be performed during the calculations of sizing of distributed generation.

## References

1. N. Acharya, P. Mahat, and N. Mithulananthan, *Int. J. Elec. Power.*, **28**, pp. 669-678, (2006)
2. M. Aman, G. Jasmon, H. Mokhlis, and A. Bakar, *Int. J. Elec. Power.*, **43**, pp. 1296-1304, (2012)
3. P. Chiradeja and R. Ramakumar, *IEEE T. Energy. Conver.*, **19**, pp. 764-773, (2004)
4. S. Elsaiah, M. Benidris, and J. Mitra, *IET Gener. Transm. Dis.*, **8**, pp. 1039-1049, (2014)
5. D. Q. Hung, N. Mithulananthan, and R. Bansal, *IEEE T. Energy. Conver.*, **25**, pp. 814-820, (2010)
6. S. G. Naik, D. Khatod, and M. Sharma, *Int. J. Elec. Power.*, **53**, pp. 967-973, (2013)
7. M. Shahzad, I. Ullah, P. Palensky, and W. Gawlik, "*Analytical approach for simultaneous optimal sizing and placement of multiple Distributed Generators in primary distribution networks*," in *Industrial Electronics (ISIE), 2014 IEEE 23rd International Symposium*, pp. 2554-2559 (2014)
8. M. W. Younas, "*SAARC Perspective Workshop on the Past, Present and Future of High Voltage DC (HVDC) Power Transmission*," Available at: <http://www.saarcenergy.org/wp-content/uploads/2016/03/6.-Pakistan.pdf> (2015).
9. A. E. D. B. (AEDB), "Available online at: <http://www.aedb.org/>."
10. Q.-e.-A. S. P. P. Limited, "Available online: <http://www.qasolar.com/>."
11. Q.-e.-A. S. P. P. L. Generation Licence, "Available online at: <http://www.nepra.org.pk/Licences/Generation/RE-2006/Quaid-e-Azam%20Solar/LAG-252%20GL%20of%20Quaid-e-Azam%20Solar%2026-06-2014%207212-17.PDF>."
12. N. S. R. D. (NSRDB), "Available online at: <https://nsrdb.nrel.gov/>."
13. D. K. Khatod, V. Pant, and J. Sharma, *IEEE T. Power Syst.*, **28**, pp. 683-695, (2013)
14. Y. Atwa, E. El-Saadany, M. Salama, and R. Seethapathy, *IEEE T. Power Syst.*, **25**, pp. 360-370, (2010)
15. J.-H. Teng, S.-W. Luan, D.-J. Lee, and Y.-Q. Huang, *IEEE T. Power Syst.*, **28**, pp. 1425-1433, (2013)
16. M. Fan, V. Vittal, G. T. Heydt, and R. Ayyanar, *IEEE T. Power Syst.*, **27**, pp. 2251-2261, (2012)

17. D. Q. Hung, N. Mithulananthan, and K. Y. Lee, IEEE T. Power Syst., **29**, pp. 3048-3057, (2014)
18. S. Naik, D. Khatod, and M. Sharma, "Sizing and siting of distributed generation in distribution networks for real power loss minimization using analytical approach," in 2013 International Conference on Power, Energy and Control (ICPEC), pp. 740-745 (2013)
19. R. Chang, N. Mithulananthan, and T. Saha, "Novel mixed-integer method to optimize distributed generation mix in primary distribution systems," in 21st Australasian Universities Power Engineering Conference (AUPEC), pp. 1-6 (2011)
20. D. Q. Hung and N. Mithulananthan, "An optimal operating strategy of DG unit for power loss reduction in distribution systems," in 7<sup>th</sup> IEEE International Conference on Industrial and Information Systems (ICIIS), pp. 1-6 (2012)
21. B. Venkatesh, R. Ranjan, and H. Gooi, IEEE T. Power Syst., **19**, pp. 260-266 (2004)
22. D. Q. Hung, N. Mithulananthan, and R. Bansal, Int. J. Amb. Energy, **36**, pp. 123-131, (2015)
23. T. Gözel and M. H. Hocaoglu, Electr. Pow. Syst. Res., **79**, pp. 912-918, (2009)
24. A. Mecke, I. Lee, J.R. Baker jr., M.M. Banaszak Holl, B.G. Orr, Eur. Phys. J. E **14**, 7 (2004)
25. L. T. De Luca, *Propulsion physics* (EDP Sciences, Les Ulis, 2009)

For journal abbreviation, you can check it at this website:

[http://images.webofknowledge.com/images/help/WOS/B\\_abrvjt.html](http://images.webofknowledge.com/images/help/WOS/B_abrvjt.html)